

Improvement of IR Pyroelectric Detector Performance in THz Range Using Wavelength-Scale Sphere-Based Terajet Effect

Oleg V. Minin¹, Igor V. Minin^{1, *}, Yanfeng Li^{2, *}, and Jianguang Han²

Abstract—An infrared (IR) pyroelectric detector for applying to the terahertz (THz) waveband that uses diffraction-limited focusing of the THz beam on the sensitive area of the detector is studied. The signal to be detected is coupled to the optical window of the detector through a two-wavelength diameter polytetrafluoroethylene spherical particle-lens based on the terajet effect. We have experimentally demonstrated an enhancement of the IR detector sensitivity by 5.6 dB at 0.2 THz without degradation of the noise equivalent power value. The results show that the proposed method could be applied to increase the sensitivity of various commercial IR sensors in the THz range, requiring no modification of the internal structure and may be applied also to acoustics and plasmonics.

1. INTRODUCTION

Terahertz (THz) waves have recently received unprecedented interest in product quality control, medicine, biology, chemical composition or water content analysis, 5G and 6G communications, nondestructive testing, and homeland security applications, to name a few [1–15] that cannot be achieved in the optical or infrared (IR) electromagnetic bands.

Golay cell [16] is a device commonly used for THz radiation detection. Bolometers are cooled and highly sensitive detectors in which the conductivity of the material changes with temperature induced by the THz radiation. Uncooled pyroelectric detectors (PDs), in which the output current is proportional to the rate of change in temperature of the film material [17], have some important advantages. Several types of special THz PDs have been developed in the last decade. A PD based on lithium tantalate crystal and film was considered in [18]. A tetraaminodiphenyl-based PD was investigated in [19], and a THz PD based on a pyroelectric polyvinylidene fluoride (PVDF) film coated with a metal oxide layer was developed in [20, 21]. It has been shown that the thickness of the pyroelectric film should be reduced to reduce the noise equivalent power (NEP) value. However, all these and other similar developments require either a new detector design or the replacement of the material in the existing commercial detector. Moreover, the present PDs designed especially for THz waves are still expensive.

On the other hand, PDs are widely used in the IR range and are produced by industry. Today IR PDs are one of the best devices in uncooled IR detectors, providing a high efficiency of detection of the illuminating radiation, relative short response time, high signal-to-noise ratio, low cost, and high reliability [22–25].

A THz detector based on an IR PD (LHI778, Perkinelmer), initially designed for the wavelength range of 7–14 μm and used in THz imaging applications, was studied in [26]. A special amplification circuit to amplify and capture the signal from the sensor was designed. A responsivity about 1200 V/W at 1.89 THz was achieved. But direct application of conventional IR PDs to the THz waveband faces the problem of decreasing detection sensitivity.

Received 19 July 2021, Accepted 3 November 2021, Scheduled 8 November 2021

* Corresponding authors: Yanfeng Li (yanfengli@tju.edu.cn), Igor V. Minin (prof.minin@gmail.com).

¹ Tomsk Polytechnic University, Lenin Avenue 30, Tomsk 634050, Russia. ² Center for Terahertz Waves and College of Precision Instrument and Optoelectronics Engineering, Key Laboratory of Optoelectronic Information Technology (Ministry of Education), Tianjin University, Tianjin 300072, China.

However, it is found that the commercial IR MG-30PD [27] is a good substitute for special THz detectors. Though it is designed for IR radiation, it retains good sensitivity at THz frequencies. A single-element MG-30 PD has a response within the radiation wavelength range of 3–20 μm and is based on a free organic film of the PVDF type [21]. A sensor sensitive area of $1 \times 1 \text{ mm}$ ensures that the sensitivity threshold in the IR range is lower than $5 \times 10^{-10} \text{ W} \times \text{Hz}^{1/2}$, and the volt-watt sensitivity is greater than 10^5 V/W [28].

To enhance the PD performance in the millimeter-wave band, the combination of an MG-33 detector, originally designed for sensing IR radiation, with a metasurface-enabled absorber was considered in [29]. The differences between MG-33 and MG-30 IR detectors are the standard package and window diameters (KT-3 package and window diameter of 3.5 mm for MG-33). Efficient frequency- and polarization-selective detection of electromagnetic waves within the frequency band of 100–180 GHz was demonstrated with a degradation of the NEP value by a factor of 2. However, this scheme required a change in both the design of the detector itself (the diameter of the optical window was specially increased from 3.5 mm to 5 mm in [29]) and the development of a new absorber, which is far from always available to the common user. In addition, due to the nature of the metasurface, the detector has a pronounced resonance character.

The aim of this work is to demonstrate the possibility of effective use of commercially available IR PDs in the THz range without changing their internal design.

One of the new approaches to increasing the sensitivity of THz detectors is based on the so-called terajet effect [30–33]. It is based on a reduction of the focused beam caustic size up to the sub-diffraction value at a distance close to the shadow surface of a wavelength-scale particle-lens made from a conventional dielectric material [34]. The effect of such a dielectric particle-lens on the THz wave is similar to that of a photonic nanojet, which was first discovered in optics and consists of subwavelength focusing of a plane wavefront incident on a dielectric particle near its shadow surface. It has recently been demonstrated that placing a dielectric cube in front of the sensitive area of a strained silicon field effect transistor [35, 36] and a point contact detector [37] allows to increase the sensitivity of the THz detectors due to the localization of the incident radiation with a slight decrease of the NEP value. In this work, we demonstrate that the same method allows to increase the sensitivity of commercial IR detectors in the THz range for room temperature operation.

2. EXPERIMENTAL SETUP

The basic scheme of the commercial MG-3PD combined with the sensitivity-enhancing dielectric particle is depicted in Fig. 1(a). To produce the terajet effect, we attached a wavelength-scale spherical dielectric particle directly to the PD window, which is made of germanium and has a thickness around $h = 110 \mu\text{m}$. The MG-30 sensor in the standard 1203.15-1 package [27], which contains a primary amplifier located on the sensor chip, is shown in Fig. 1(b).

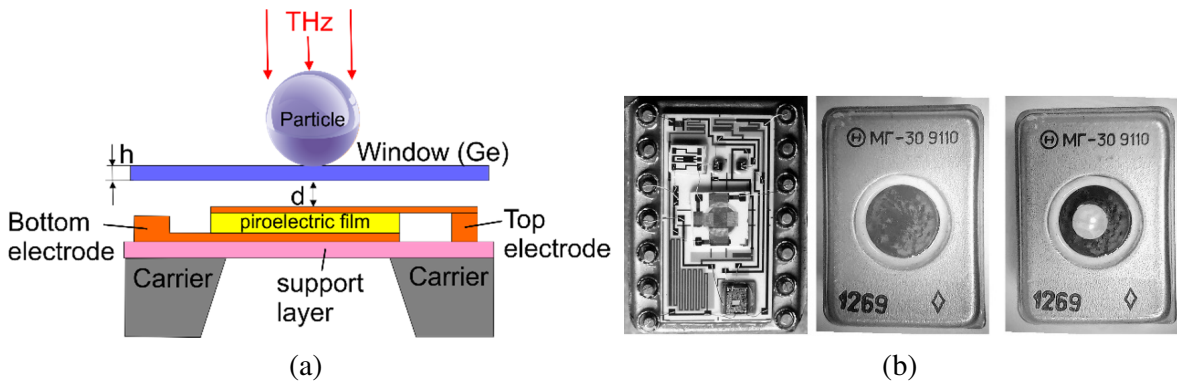


Figure 1. (a) Schematic of the commercial MG-30 PD combined with the dielectric particle (not to scale); (b) MG-30 detector in the standard 1203.15-1 package with a standard window of diameter of 6.5 mm.

To increase the coupling efficiency of the PD with the THz radiation source (at a wavelength of 1.5 mm, which corresponds to a frequency of about 0.2 THz), we used the terajet formed by a polytetrafluoroethylene (PTFE) sphere (commercially available from Goodfellow) with a two-wavelength diameter instead of a cubic particle, which has to be specially manufactured. The refractive index of PTFE is $n = 1.41$ [38–40], and the beam waist of the terajet (in full width at half maximum) for this dimension of the PTFE sphere is about 0.5 wavelengths. The maximum of the field intensity enhancement was observed at a distance about 0.7 mm from the shadow surface of the particle. When the features of the construction assembly of the PD shown in Fig. 1(a) (the minimal distance between the shadow surface of the window and sensitive element is not equal to zero and has a fixed value d , determined by the manufacturer technology) are taken into account, the focal distance of the terajet is selected to be equal to half of a wavelength (Table 1).

Table 1. Simulation results of focal length of spherical particle versus diameter.

D/λ	2	3	4
F/λ	0.47	0.52	0.58

As the radiation source, a backward-wave oscillator (BWO) [41] (“OV-1” type, Istok Co.) was chosen for its special features such as stability, a relative high output power (6–15 mW), good wavefront quality, and frequency tunability from 177 to 260 GHz.

The measurements (Fig. 2) show a linear dependence of the voltage (U) on the power at $\lambda = 1.5$ mm (this value gives the maximum output power from the BWO). A certified attenuator was used to control the emitted power sent to the receiver. The method for measuring NEP was similar to that described in [29].

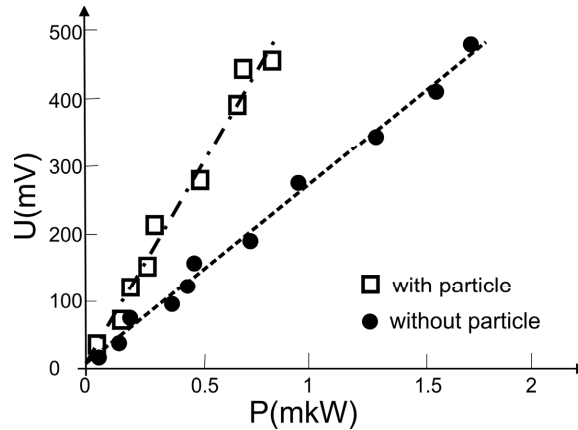


Figure 2. Voltage-power characteristics of the MG-30 PD measured at a wavelength of $\lambda = 1.5$ mm. $NEP \approx 6 \times 10^{-9} \text{ W} \times \text{Hz}^{-1/2}$, and $S_{\text{ens}} \approx 2.6 \times 10^5 \text{ V/W}$ for the PD without the particle.

The idea of this configuration is to exploit the dielectric PTFE particle that has a wavelength-scale diameter to concentrate the illuminating THz waves into the sensitive area of the PD with a diffraction-limited size. This allows to increase the intensity of the signal to be measured such that the signal-to-noise ratio can be improved. In the experiment, the PTFE particle was directly placed and glued onto the optical window of the PD. The horn antenna of the BWO was placed at a distance of approximately 220 mm from the detector window (which corresponded to the far-field condition) to form a quasi-plane wavefront.

3. EXPERIMENTAL RESULTS

Figure 3 shows the measured photo-response without the particle (black curve) and with the sphere (red curve). To demonstrate the sensitivity enhancement, the detector was excited by the source at its

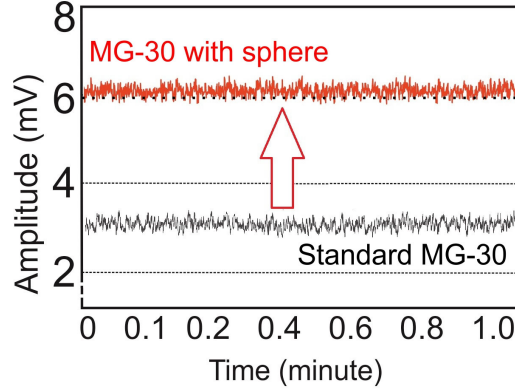


Figure 3. Measured amplitudes with/without the PTFE sphere at 0.2 THz.

lowest power when the signal from the receiver (without the particle) was at the noise level. Then we placed the PTFE particle in front of the detector and observed the increase in the signal and the noise level. The measured amplitude with the sphere placed in front was 6.2 ± 0.06 mV, which was 5.6 dB higher than that from the standard MG-30 PD without the enhancer. The standard error was calculated from nine distinct measurements and a Student's t-distributions coefficient [42] of 2.132, corresponding to a 90% two-sided confidence interval. The standard deviations of the amplitude were measured for the cases without and with the PTFE particle, respectively. These results indicate that the proposed technique could enhance the detected THz intensity by 5.6 dB at 0.2 THz for the MG-30 PD.

4. CONCLUSION

It is demonstrated that the commercial IR PD performance can be improved in the THz range using the terajet effect based on a commercially available non-resonant spherical dielectric particle. A gain enhancement about 6 dB was experimentally observed at 0.2 THz for a commercial IRMG-30 PD without degradation of the NEP value. The research results confirm the prospects of using commercial IR detectors in the THz range [26, 43, 44] while requiring no changes in their design. The entire setup offers a cost-effective solution for sensitivity enhancement of IR PDs in the THz range, which can be applied in many fields, including imaging systems [7], THz wireless communications [9, 45], etc. This method of increasing the sensitivity of commercial sensors can also be applied to both acoustic [46] and plasmonic [47] devices.

ACKNOWLEDGMENT

This work was partially supported by TPU development program and the National Natural Science Foundation of China (Grant No. 61935015).

REFERENCES

1. Dhillon, S. S., M. S. Vitiello, E. H. Linfield, et al., "The 2017 terahertz science and technology roadmap," *Journal of Physics D: Applied Physics*, Vol. 50, No. 4, 043001, 2017.
2. Kawase, K., O. Yuichi, W. Yuuki, et al., "Non-destructive terahertz imaging of illicit drugs using spectral fingerprints," *Optics Express*, Vol. 11, No. 20, 2549–2554, 2003.
3. Ferguson, B., S. Wang, D. Gray, et al., "T-ray computed tomography," *Optics Letters*, Vol. 27, No. 15, 1312–1314, 2002.
4. Federici, J. and L. Moeller, "Review of terahertz and subterahertz wireless communications," *Journal of Applied Physics*, Vol. 107, No. 11, 111101, 2010.
5. Siegel, P. H., "Terahertz technology in biology and medicine," *IEEE Transactions on Microwave Theory and Techniques*, Vol. 52, No. 10, 2438–2447, 2004.

6. Hu, B. B. and M. C. Nuss, "Imaging with terahertz waves," *Optics Letters*, Vol. 20, No. 16, 1716–1718, 1995.
7. Chernomyrdin, N. V., A. S. Kucheryavenko, G. S. Kolontaeva, et al., "A potential of terahertz solid immersion microscopy for visualizing sub-wavelength-scale tissue spheroids," *Proceedings of SPIE*, Vol. 10677, 106771Y, 2018.
8. Minin, I. V. and O. V. Minin, "System of microwave radiovision of three-dimensional objects in real time," *Proceedings of SPIE*, Vol. 4129, 616–619, 2000.
9. Samura, Y., K. Horio, V. B. Antipov, et al., "Characterization of mesoscopic dielectric cuboid antenna at millimeter-wave band," *IEEE Antennas and Wireless Propagation Letters*, Vol. 18, No. 9, 1828–1832, 2019.
10. Samura, Y., K. Yamada, O. V. Minin, et al., "High-gain and low-profile dielectric cuboid antenna at J band," *14th European Conference on Antennas and Propagation (EuCAP)*, 2020.
11. Owda, A. Y., N. Salmon, A. J. Casson, et al., "The reflectance of human skin in the millimeter-wave band," *Sensors*, Vol. 20, No. 5, 1480, 2020.
12. Ajito, K. and Y. Ueno, "THz chemical imaging for biological applications," *IEEE Transactions on Terahertz Science and Technology*, Vol. 1, No. 1, 293–300, 2011.
13. Taylor, Z., J. Garritano, S. Sung, et al., "THz and mm-wave sensing of corneal tissue water content: *in vivo* sensing and imaging results," *IEEE Transactions on Terahertz Science and Technology*, Vol. 5, No. 2, 184–196, 2015.
14. Pagano, M., L. Baldacci, A. Ottomaniello, et al., "THz water transmittance and leaf surface area: An effective nondestructive method for determining leaf water content," *Sensors*, Vol. 19, No. 22, 4838, 2019.
15. Zang, Z., J. Wang, H. L. Cui, et al., "Terahertz spectral imaging based quantitative determination of spatial distribution of plant leaf constituents," *Plant Methods*, Vol. 15, No. 1, 106, 2019.
16. Golay, M. J. E., "Theoretical consideration in heat and infrared detection, with particular reference to the pneumatic detector," *Review of Scientific Instruments*, Vol. 18, No. 5, 347–356, 1947.
17. Stenger, V., M. Shnider, S. Sriram, et al., "Thin film lithium tantalate (TFLT) pyroelectric detectors," *Proceedings of SPIE*, Vol. 8261, 82610Q, 2012.
18. Wang, J., J. Gou, and W. Li, "Preparation of room temperature terahertz detector with lithium tantalate crystal and thin film," *AIP Advances*, Vol. 4, No. 2, 027106, 2014.
19. Paulish, A., A. V. Gusachenko, A. O. Morozov, et al., "Characterization of tetraaminodiphenyl-based pyroelectric detector from visible to millimeter wave ranges," *Optical Engineering*, Vol. 59, No. 6, 061612, 2020.
20. Müller, R., W. Bohmeyer, M. Kehrt, et al., "Novel detectors for traceable THz power measurements," *Journal of Infrared, Millimeter, and Terahertz Waves*, Vol. 35, No. 8, 659–670, 2014.
21. Müller, R., B. Gutschwager, J. Hollandt, et al., "Characterization of a large-area pyroelectric detector from 300 GHz to 30 THz," *Journal of Infrared, Millimeter, and Terahertz Waves*, Vol. 36, No. 7, 654–661, 2015.
22. Rogalski, A., *Infrared Detectors*, 2nd Edition, CRC Press, 2010.
23. Neumann, N. and V. Banta, "Comparison of pyroelectric and thermopile detectors," *Proceedings of AMA Conferences 2013*, 139–143, 2013.
24. Zhao, J., R. Zhu, J. Chen, et al., "Enhanced temperature stability of compensated pyroelectric infrared detector based on Mn:PMN-PT single crystals," *Sensors and Actuators A: Physical*, Vol. 327, 112757, 2021.
25. Ng, D. K. T., C. P. Ho, T. T. Zhang, et al., "CMOS compatible MEMS pyroelectric infrared detectors: From AlN to ScAlN," *Proceeding of SPIE*, Vol. 11697, 116970N, 2021.
26. Yang, J., X. Gong, and Y. D. Zhang, "Research of an infrared pyroelectric sensor based THz detector and its application in CW THz imaging," *Proceedings of SPIE*, Vol. 7385, 738521, 2009.
27. Vostok Science and Production Enterprise, <http://www.nzpp.ru/product/gotovye-izdeli/fotopriemnye-ustroystva/MG30.pdf>.

28. Ivanov, S. D. and E. G. Kostsov, "Thermal detectors of uncooled multi-element infrared imaging arrays. I. Thermally insulated elements," *Optoelectronics, Instrumentation and Data Processing*, Vol. 51, No. 6, 601–608, 2015.
29. Kuznetsov, S., A. Paulish, M. Navarro-Cía, et al., "Selective pyroelectric detection of millimetre waves using ultra-thin metasurface absorbers," *Scientific Reports*, Vol. 6, 21079, 2016.
30. Pacheco-Pena, V., M. Beruete, I. V. Minin, et al., "Terajets produced by dielectric cuboids," *Applied Physics Letters*, Vol. 105, No. 8, 084102, 2014.
31. Minin, I. V. and O. V. Minin, "Terahertz artificial dielectric cuboid lens on substrate for super-resolution images," *Optical and Quantum Electronics*, Vol. 49, No. 10, 326, 2017.
32. Yue, L., B. Yan, J. N. Monks, et al., "A millimetre-wave cuboid solid immersion lens with intensity-enhanced amplitude mask apodization," *Journal of Infrared, Millimeter, and Terahertz Waves*, Vol. 39, No. 6, 546–552, 2018.
33. Pham, H., S. Hisatake, I. V. Minin, et al., "Three-dimensional direct observation of Gouy phase shift in a terajet produced by a dielectric cuboid," *Applied Physics Letters*, Vol. 108, No. 19, 191102, 2016.
34. Minin, I. V., O. V. Minin, and Y. E. Geints, "Localized EM and photonic jets from non-spherical and non-symmetrical dielectric mesoscale objects: Brief review," *Annalen der Physik*, Vol. 527, Nos. 7–8, 491–497, 2015.
35. Minin, I. V., O. V. Minin, J. Delgado-Notario, et al., "Improvement of a terahertz detector performance using the terajet effect in a mesoscale dielectric cube: Proof of concept," *Physica Status Solidi-Rapid Research Letters*, Vol. 14, No. 5, 1900700, 2020.
36. Minin, I. V., O. V. Minin, J. Salvador-Sanchez, et al., "Responsivity enhancement of a strained silicon field effect transistor detector at 0.3 THz using the terajet effect," *Optics Letters*, Vol. 46, No. 13, 3061–3064, 2021.
37. Minin, O. V., I. V. Minin, Y. M. Meziani, et al., "Improvement of a point-contact detector performance using the terajet effect initiated by photonics," *Optical Engineering*, Vol. 60, No. 8, 082005, 2020.
38. D'Angelo, F., Z. Mics, M. Bonn, et al., "Ultra-broadband THz time-domain spectroscopy of common polymers using THz air photonics," *Optics Express*, Vol. 22, No. 10, 12475–12485, 2014.
39. Folks, W. R., S. K. Pandey, and G. Boreman, "Refractive index at THz frequencies of various plastics," *Optical Terahertz Science and Technology, OSA Technical Digest Series*, paper MD10, 2007.
40. Jin, Y. S., G. J. Kim, and S. G. Jeon, "Terahertz dielectric properties of polymers," *Journal of the Korean Physical Society*, Vol. 49, No. 2, 513–517, 2006.
41. Kompfner, R. and N. Williams, "Backward-wave tubes," *Proceedings of the IRE*, Vol. 41, No. 11, 1602–1611, 1953.
42. Hotelling, H., "The generalization of student's ratio," *Breakthroughs in Statistics*, S. Kotz, N. L. Johnson (Eds), Springer, New York, NY, 1992.
43. Dooley, D., "Sensitivity of broadband pyroelectric terahertz detectors continues to improve," *Laser Focus World*, Vol. 46, No. 5, 49–53, 2010.
44. Dégardin, A., V. Jagtap, M. Razanoelina, et al., "Y-Ba-Cu-O semiconducting pyroelectric thermal sensors: Design and test of near-infrared amorphous thin film detectors and extension to antenna-coupled THz devices," *Proceedings of SPIE*, Vol. 11164, 1116409, 2019.
45. Yamada, K., Y. Samura, O. V. Minin, et al., "Short-range wireless transmitter using mesoscopic dielectric cuboid antenna in 300-GHz Band," *Proceeding of 50th European Microwave Conference (EuMC)*, 195–198, 2021.
46. Tarrazó-Serrano, D., C. Rubio, O. V. Minin, et al., "Ultrasonic focusing with mesoscale polymer cuboid," *Ultrasonics*, Vol. 106, 106143, 2020.
47. Minin, I. V., O. V. Minin, I. A. Glinskiy, et al., "Plasmonic nanojet: An experimental demonstration," *Optics Letters*, Vol. 45, No. 12, 3244–3247, 2020.